AN OVERVIEW OF THE MATHEMATICAL MODELLING OF REHEATING FURNACES

Abstract

Over the past 30 years, great efforts have been made to study the heating properties of sheet/sheets in various furnaces with an incipient thermal field. Numerous mathematical modelling studies related to industrial scales have been reported. Mathematical modelling using is used to solve the heat transfer equations for conduction and radiation using finite volume formulation techniques. A mathematical heat transfer model uses a controlled volume and controlled angle approximation to solve the radiative heat transfer equation to predict the radiative heat flux across the plate surface. Another method is to correlate different approaches to solve conduction and radiation problems to predict plate temperature profiles and has worked on real-time simulations of online models involving graphical user interfaces. There has been a considerable research on various modelling techniques and methodologies, such as turbulent jet flow of fuel gases, convective and radiative phenomena in furnaces, slab conduction phenomena, and weighted sum models of gray gases.

Keywords: Reheating furnaces, Mathematical modelling, Steelmaking, Steel slabs

Authors

Abhinav Maurya
Department of Metallurgical and Materials Engineering
Indian Institute of Technology Ropar
Punjab, India.

Prvan Kumar Katiyar
Department of Metallurgical and Materials Engineering
National Institute of Technology Srinagar
Jammu and Kashmir, India.

Prince Kumar Singh
Department of Metallurgical and Materials Engineering
Indian Institute of Technology Ropar
Punjab, India.
princeks@iitrpr.ac.in

I. INTRODUCTION

Reheating furnaces in steel mills heats plates, ingots, billets and blanks to achieve uniform and optimal rolling temperatures. Heating furnaces can be divided into intermittent (batch) or continuous. Continuous types include pusher furnaces, rotary furnaces, moving beams, and roller hearths. Aviary heaters are considered "state of the art" in all of these situations. These furnaces are fired directly from gas and the fuel is natural gas, coke gas, blast furnace exhaust and mixtures thereof. Moving beam heating furnaces are used for heating steel plates/bills of various sizes and dimensions. The grater/batter can be charged at ambient temperature (from the tank) or warm (straight from the continuous charger) as well as at room temperature. Most reheat operations often have different sheet/sheet grades, but the sheet size is mostly constant. As the steel plates passes through the furnace and other temperature zones, the temperature increases depending on the furnace temperature zone. However, the temperature rates are higher in the preheat and reheat zones due to the firing rates in the individual furnace zones. The low temperature (plate temperature is usually 27 °C) is exposed to a high temperature furnace (1260-1280 °C). A low heating rate prevents the development of thermal stresses. The plate is then strongly heated to an annealing zone where the absorption temperature is maintained to achieve a uniform plate temperature for further rolling. The uniformity in the grains sizing along the entire length of the steel slabs/billets is affected by the quality of heating and the effectiveness of the reheating process, and it might have an impact on the mechanical qualities of the completed goods. The heating quality of the slabs in industrial reheating processes depends on a variety of combustion process factors, including the burner schematic, air-to-gas ratio, furnace structure, and refractory materials[1].

1. **Reheating Furnaces in Steel Industries:** Reheating activities are primarily intended to achieve homogeneous, ideal slab/billet temperatures and increase the materials' softness, which is suited for rolling operations. The fuel feeding rate and air-to-fuel mixture in the burners in the various zones of the reheating furnace are used to achieve the ideal rolling temperature. The length of flames and amount of time that hot flue gas interacts with the stock determine the heating effectiveness of the reheating furnace. Fuel/air flow rate determines the flame's length[1]. The thermo-physical characteristics of the materials, such as their thermal conductivity and specific heat, affect how quickly steel slabs and billets heat up.A direct contact with flames, hot furnace walls, and radiation from hot combustion gases, steel slab temperature is significantly larger on the surface. Radiation is the primary route of heat transfer in a reheating furnace. According to length of the reheating furnace, the furnace is separated into three to five temperature zones, with the temperature rising along the furnace's longitudinal direction.

   The temperature of steel slabs is increased to necessary range within the reheating furnace to achieve the plastic characteristics needed for rolling operation. Reheating furnaces are a crucial component of rolling mills. The primary goal of heating materials is to soften them for rolling operations, which is done by setting an initial temperature that is sufficiently high so that rolling may take place in a fully austenitic temperature range[1][2][3][4].Combustible gases like O_2, CO_2, H_2O, etc. react with the steel slab surface temperature as it rises. The steel slabs develop an oxide coating (scale) on their surface as a result of the furnace's oxidising environment. The steel slabs' or bills' surface temperature, time spent in the reheating furnace, and the abrasiveness of the oxidising environment all affect how thick the oxide layer is. In a rolling mill, which is a crucial component of a steel plant, slabs are heated to precise target temperatures in

reheating furnaces. Since heating slabs uses a lot of energy, it is preferable to manage the temperatures of the discharged slabs to heat them precisely to the desired degree in order to save energy.[3].

Rotatory hearth, walking hearth, pusher type, continuous recirculating bogie and walking beam furnace type are the five categories into which continuous type reheat furnaces can be separated. Pusher type and walking beam type are the most frequently used reheating furnaces are used to reheat billets, ingots, and slabs with various beginning thermal fields. The technique of walking beam type reheating furnace (WB furnace) is crucial for having seamless functioning [5]. The rolled product's quality, manufacturing rate, energy use, pollutants, and economics are all determined by the design elements and operating conditions. Present-day WB furnace consistently and uniformly heat slabs, blooms, and billets to the necessary temperature while minimising the production of skid marks[4].It can be separated into three zones – preheating, heating and soaking; or five zones – non-firing, charging, preheating, heating and soaking. Steel slabs charged into the non-firing zone are transported to the following succeeding zone on the fixed beam by a walking beam at a set velocity. The furnace's overall length is 35 to 40 metres, and its height varies in each zone thanks to slopes that connect the top and its dam-shaped bottom. The size of the reheating furnace determines the number of slabs and burners. With dimensions of 9 metres in length, 1.16 metres in width, and 0.23 metres in height, reheating furnaces typically heat 28 to 30 slabs at once, with a 0.2 metre space between each slab. In the reheating furnace, the slab stays there for 180–200 minutes. A total of 50 burners were installed in the reheating furnace, with 24 axial burners in the upper zone and 26 side burners in bottom zone.
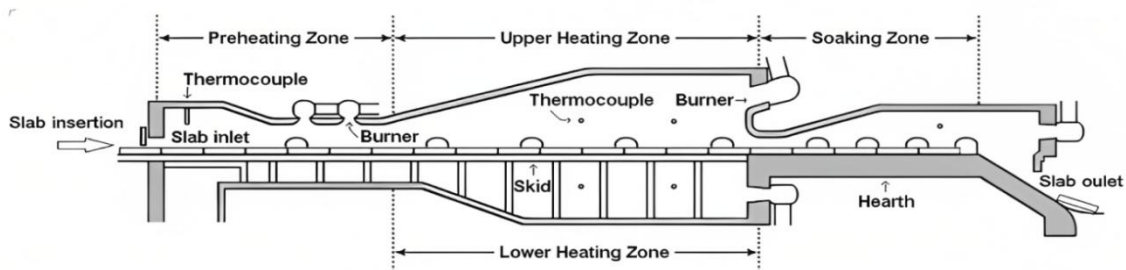

Figure 1: Schematic of pusher type reheating furnace[6]
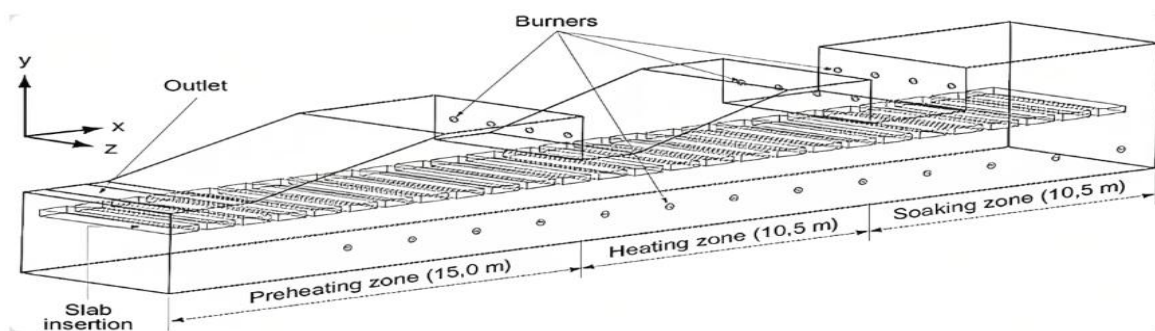
Figure 2: Schematic of Walking beam type reheating furnace without skid beam arrangement[7].

2. **Heat Transfer Modes in Reheating Furnaces:** It is well known that the reheating furnaces use the three traditional heat transfer mechanisms to bring slabs up to temperature: conduction, convection, and radiation. In a reheating furnace, radiation is the primary route of heat transmission. This is because convection heat transfer coefficient and temperature difference between slabs and combustion gases are both important factors in convection heat transmission, whereas in radiation heat flow rate is directly related to the temperature raised to the fourth power. As a result, convection has little impact on slab heating. Combustible gas composition, adiabatic flame temperature, slab emissivity, and reflectivity of the refractory walls of the reheating furnace's various zones are the key factors affecting radiation heat transmission. The turbulent combustion model predicts the impact of the temperature characteristic [2][3][4]. The weighted-sum-of-gray-gases (WSGGM) model, which determines the absorption coefficient for gas molecules, only considers participating molecules like CO_2 and H_2O due to their strong spectrum radiative properties. For better accurate prediction of gas radiation, this model is more precise and pragmatic than any grey gas model [8].
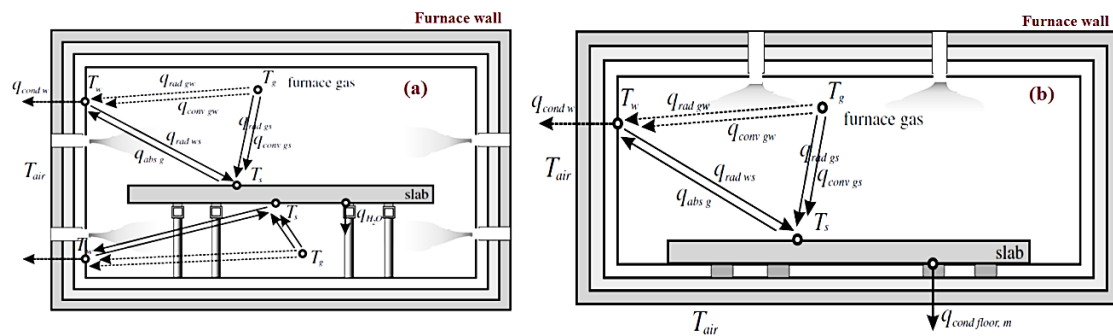
Figure 3: Heat transfer phenomena in reheating furnace (a) heat transfer in preheating, heating zones, and (b) soaking zone[2][9].

3. **Effect of Flame Characteristics on Heat Transfer:** It is well known that heating steel slabs or a charge in a reheating furnace mostly involves the transfer of heat by radiation. The reheat furnace's flame, which has the maximum temperature, radiates heat to the furnace wall and steel surface. As a result, the heat transfer is greatly affected by the form, length, and properties of the flame. The fuel type such as coke oven gas (COG) and blast furnace gas (BFG), the burner design, and various fuel and air flow rates can all affect it. Good mixing produces a high-quality flame; as a result, short, bushy flames are produced by high turbulence velocity, which increases the rate of convective heat transfer inside the furnace enclosure. A longer, narrow flame will develop if the fuel and oxidizer are not mixed thoroughly or quickly enough. Higher throughput and optimal reheating furnace efficiency result from using the appropriate adiabatic flame temperature [1].

4. **Energy Optimization in Reheating Furnaces:** The size and design of the reheat furnace are crucial when reheating slabs (also called charge or load). The design should be in made in order to maximise quantity of charge that can be heated to a uniform temperature, suitable for subsequent operation, in a given length of time with the least amount of fuel and labour. The encapsulation of the following criteria can be used to complete this task[3][4][10]:

- Calculating the amount of heat to be applied to the charge.
- The production of sufficient heat inside the furnace to warm the charge and offset any potential losses.
- The transport of heat from furnace enclosure to charge surface.
- Steel stock's stock temperature consistency.
- Lowering the reheat furnace's heat losses.

5. **Efficiency Difficulties in Reheating Furnace:** Various restrictions and complexities might reduce performance and efficiency while reheating is being done in a reheat furnace. Steel stock/charge and combustible gases move in different directions during the reheating process, which causes fuel-fired reheating furnaces to frequently have efficiency issues. Hot flue gases and a little amount of heat loss via the furnace wall are the two main sources of heat loss in reheat furnaces. Heat loss through the hot flue gases and the furnace wall likewise rises as the temperature of the reheat furnace rises. Running a reheat furnace at rated capacity with the same grade of steel, similar composition, beginning thermal profile of charge, and uniform size is the optimum scenario. However, in reality, this does not take place. The residence period of the reheat furnace, which can impact furnace efficiency, may be interrupted by the composition of the fuel and rolling delays [3].

6. **Oxidation Loss or Burning of Materials in Reheating Furnace:** Steel slabs and billets oxidise at the surface while being heated in a reheat furnace. The high temperature and oxidising environment of the reheat furnace are the primary causes of scale growth on the slab surfaces. Higher temperatures cause oxygen to break into ions, which controls the diffusion of oxygen. With rising steel surface temperatures and partial oxygen and carbon dioxide enrichment in fuel, scale thickness rises. Oxidation loss of the materials is also caused by a delay in rolling operation and an extended residence period of the charge. Iron oxide can occur in the presence of hot combustion gases. It's crucial to predict the oxidation kinetics in a reheating furnace in order to determine the steel yield loss. Along with energy losses, the yield loss during the reheating process varies from 1.50% to 2.50% by weight. By reducing the extra air during burning, we can prevent the loss of 35% of the steel owing to scaling. The burning and melting of grain boundary caused by high temperature oxidation of steel's surface can reduce the material's strength and may result in rolling cracks.

   Metal oxidation is directly influenced by temperature; at 900°C, oxygen content has little effect on steel oxidation; nevertheless, beyond 1200°C, oxygen content in reheat furnace increases from 0.30% to 2.9%, increasing the oxidation rate by 50%. Any additional increases in oxygen levels above 3% will only have a minor impact on oxidation[4][11][12].In the presence of hot oxidising combustible gases, slabs or bills are heated in the furnace at a higher temperature (1250°C). At such temperatures, carbon oxidises quickly than iron. Decarburization of the charge from the surface layer might therefore have an impact on the mechanical characteristics of finished goods. Diffusion, a thermally stimulated process, regulates the decarburization process. Reducing the furnace's dwell duration and excessive temperature can reduce amount of carbon that diffuses from the core to surface[4].

7. **Advantages of Using Oxy-Fuel Combustion in Reheating Furnace:** Steel slab/billet reheating is an energy-intensive operation that demands even temperature distribution throughout the furnace's various heating zones. In oxyfuel practise, industrial-grade liquid oxygen that is vaporised to gas fully replaces air. Industrial-grade liquid oxygen is more affordable and has a purity of 90% to 93%. The technique of burning oxy-fuels has more advantages over burning air-fuels since it emits less greenhouse gases, produces less nitrogen gas, and loses less heat from the flue gas. Additionally, due to their highly spectrum radiative properties, highly radiating combustion products like CO_2 and H_2O are concentrated more in the furnace environment and contribute to radiative heat transfer inside the furnace enclosure. Oxyfuel combustion has higher heating rates, fuel savings, decreased SO_x emissions, and NO_x emissions as a result[13].
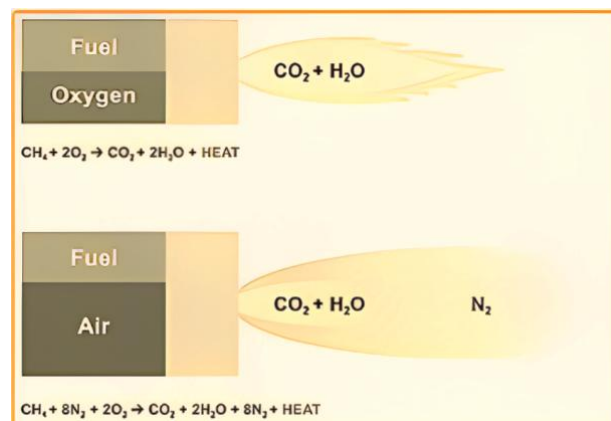
Figure 4: An assessment of oxy-fuel and fuel-air combustion[13]

In Oxy-fuel combustion, furnace gases produce CO_2 and H_2O with higher levels of radiative characteristics and specific heat and higher emission powers. Oxy-fuel burners have a substantially higher thermal efficiency (80%) than air-fuel (40–60%) burners as CO_2 and H_2O (g) enable the high heating rate and thus, decrease the time factor for scale formation. Further, there is no negative impact on scale formation on steel slabs or bills in the case of oxy-fuel combustion as the oxy-fuel environment immediately creates a thin and dense oxide layer that stops additional oxidation and scale formation on reheat steel, scale is thinner in oxy-fuel combustions. The features of scale production are also different in oxy-fuel combustions. The ability of steel slabs to absorb heat for a certain period and temperature at which steel is subjected to heat determines the practical limit to production growth. Higher production results from the steel slabs' enhanced rate of heating [4][10][11].

II. PREVIOUS STUDIES

After a thorough literature search, each feature of the reheating furnace that needs to be represented has been explained in this paper [2][3][4] using various mathematical modelling techniques. The mathematical modelling uses numerical techniques to solve the conduction and radiation transfer equation (RTE) utilising finite volume method (FVM)[14][15] so as to forecast the radiation flux falling on slab, and a conductive model to establish the temperature variation within the slab. One mathematical model is concerned with the dynamic model used to determine the temperature profile of each slab in a

continuous pusher type reheating furnace utilising real-time data, which can be accomplished using a sophisticated computer control system [16][17].For walking beam furnace type reheating furnaces (WB furnace), a mathematical solution has been developed to lower production costs and improve energy usage. It uses non-linear least squares pattern search with open-loop identification based on the controller throughout the heating curve up process. To conserve the WB furnace reheating furnace and manage the right temperature with a heating curve, they created an open close burner [18]. Using Genetic Algorithm, a mathematical model was created to estimate the WB furnace parameter. The temperature in each zone is measured to determine the best controller design. This mathematical model was employed to regulate the temperature with the aid of a controller, which can lower the pace at which the reheat furnace consumes fuel [19][20]. Due to low processing cost and a relatively straight forward technique, the total heat exchange factor method is frequently employed in mathematical models for online control [21].

In order to anticipate the heating behaviour of steel slabs or bills in reheating furnace, a number of useful mathematical models and techniques have been created and effectively applied in a variety of furnace geometries. These current studies can be divided into three groups to make things easier. The first strategy is straightforward, replicates the thermal properties of slabs, and concentrates on transient heat conduction within slabs as well as radiative heat transfer in furnace enclosure. The RTE in this model is discretized using the FVM formulation and iteratively solved with the tri-diagonal matrix algorithm (TDMA) approach. The heat conduction equation's boundary condition is the obtained heat flux. The third method makes use of real time simulation or other mathematical models based on the Monte Carlo method to ascertain view factor matrix and establish the heating properties of the slabs in reheating furnaces as well as to resolve the radiation transfer inside furnace.

Table 1: Heating Characteristics of Slabs (Heat is only Transferred By Radiation)

Residence Time (s)	Slab Exit Temperature (K)	No. of Furnace Zones	Observations	Reference
10,800.0	1474.0	5.0	The temperature of the slabs rises as their emissivity and absorption coefficients increase.	M Y Kim (2007) [22]
7424.0	1274.0	8.0	Out of four residence times (5670s, 6496s, 6960s, and 7424s), 7424s and 6960s satisfied the 26th and 28th slabs' requirements for temperature homogeneity.	S H Han et al. (2009) [23]
8448.0	1393.0	14.0	For various fuel input circumstances, the parameters of slab heating and the thermal behaviour of the furnace were examined.	S H Han et al. (2011) [24]
8448.0	1374.0-1574.0	14.0	Determine how COG and BFG will affect the heating efficiency of the reheating furnace.	S H Han et al. (2012) [25]

Table 2: Heating Characteristics of the Slabs (Heat is only Transferred By Convection and Radiation)

Residence Time (s)	Slab Exit Temperature (K)	No. of Furnace Zones	Observations	Reference
9000.0	1083.0	0.0	The ideal residence duration and the slabs' emissivity both help to increase the temperature uniformity of the slabs.	J. Harish (2005) [26]
10800.0	~1200.0	5.0	By adjusting slabs' emissivity and residence time, the skid mark effect has been studied on the slab.	J H Jang (2008) [27]
10800.0	~1200.0	5.0	Scale thicknesses are 1.75 mm and 1.55 mm on the top and bottom slab surfaces, respectively.	J H Jang (2010) [28]
10740.0	1397.0	3.0	Furnace's ideal location was determined to adjust operation parameters, i.e. slab size & temperature.	D E Lee (2011) [29]
10740.0	1444.0	3.0	Altered the furnace temperature and two separate charging temperatures to increase the uniformity of the slab's heating.	D E Lee (2013) [30]
10800.0	~1274.0	3.0	Temperature causes the scale's thickness to rise. Scales have a low thermal conductivity and a high specific heat, which prevent heat from combusting gases from transferring to the slab.	M Y Kim (2013) [31]
10800.0-16200.0	~1404.0	5.0	Increase in uniformity of slab heating with higher emissivity.	G. W. Lee (2014) [32]

Table 3: Thermal Performance of WB Furnace (Convection and Radiation are only Modes of Heat Transfer)

No. of slabs in furnace	Furnace Size (Kg)	Production Rate (Tons/hr)	Observations	Reference
-	-	-	In pusher-style reheating furnace, convection heat flux was obtained using correlations.	J. Harish (2005) [26]
29.0	456537.60	152.21	The furnace's end's slab with skid has a lower centreline temperature of 30°C.	J H Jang (2008) [27]
29.0	456537.60	152.21	Due to a varying heating rate, temperature of slab with scale was 10°C lower at reheating furnace's exit than it would be without scale.	J H Jang (2010) [28]

29.0	411876.22	138.07	By raising the furnace temperature by 20°C, the slab's thermal properties are improved.	D E Lee (2011) [29]
29.0	411876.22	138.07	Improved charging temperatures of the slab and a novel pattern of furnace temperature are used to provide improved thermal uniformity, fewer skid marks and the best residence time.	D E Lee (2013) [30]
29.0	539657.10	179.91	Parabolic law represents slab thickness, $x^2 = k_p t$.	M Y Kim (2013) [31]
22.0	–	–	Spectrum behaviours of CO_2 and H_2O combustion products in furnace are modelled using weighted-sum-of-gray-gases (WSGGM).	G W Lee (2014) [32]

III. MODELLING AND SIMULATION OF WB FURNACE

In a WB furnace, several simultaneous processes must be modelled. It is required to model the radiation-dominant processes that take place inside the reheating furnaces. To determine the radiation flux on slab surface, a radiative heat transfer model is used. Hot flammable gases, walls, flames, and slabs transfer heat by radiation. Newton's law of cooling is used to represent the heat transfer caused by convection between combustible flue gases, slabs, and furnace walls. Conductive heat transport in steel slabs and furnace walls is modelled by the transient heat conductive model. The reheating furnace's temperature, combustible gas composition, and flow field are all determined using a combustion model [10]. The turbulent model is used for modelling the turbulent nature of reactive flow by flammable hot gases inside the furnace [4].

1. **Evaluation of Several Reheat Model Types:** Various heat transfer models such as radiation heat transfer inside the reheating furnace and conductive heat transfer within the slabs have been compared on the basis of accuracy, simplicity, and computational effectiveness. To forecast the transient heat transfer properties of the slabs in a WB furnace, several heat transfer models are available. While some models are simple and accurate with minimal computing time, others are quite complicated and require a lot of computation time, while still others combine simplicity and accuracy with only a slight deviation from the other[33][7][34].

2. **Mathematical Formulation of Radiation Transfer Equation:** This study makes the assumption that only thermal radiation contributes to heat transmission to slab surfaces, and that only conduction occurs within slabs. The following transient three-dimensional heat conduction equation can be used to determine how much heat is transferred inside the steel slab.

$$\rho C \frac{\partial T}{\partial t} = \frac{\partial}{\partial x}\left(k \frac{\partial T}{\partial x}\right) + \frac{\partial}{\partial y}\left(k \frac{\partial T}{\partial y}\right) + \frac{\partial}{\partial z}\left(k \frac{\partial T}{\partial z}\right) \qquad (1)$$

Where the steel slab's density, specific heat, and conductivity are, respectively, denoted by, ρ, C and k. The boundary condition of aforementioned equation uses the radiation flux on slab surface.

$$q_{slab}^{R} = \int_{\Omega=4\pi} I(\vec{r}_w, \vec{s}) \, (\vec{s} \cdot \vec{n}_w) d\Omega \qquad (2)$$

Where, $I(\vec{r}_w, \vec{s})$ is used as the radiation intensity on slab surface $\vec{r}_w$ in direction $\vec{s}.\vec{n}_w$, Ω are unit normal vector and solid angle at the slab surface.

For a radiation dominant medium, radiation intensity at any position $\vec{r}$ along a path $\vec{s}$ within a medium having absorption, emission and scattering can be calculated by theusing the following RTE:

$$\frac{1}{\beta_0}\frac{dI(\vec{r},\vec{s})}{ds} = -I(\vec{r},\vec{s}) + (1-\omega_0)I_b(\vec{r}) + \frac{\omega_0}{4\pi}\int_{\Omega'=4\pi} I(\vec{r},\vec{s})\, \Phi(\vec{s}' \to \vec{s}) d\Omega' \qquad (3)$$

where, $\beta_o = \kappa_a + \sigma_s$ is extinction coefficient, $\omega_o = \frac{\sigma_s}{\beta_o}$ is scattering albedo, and $\Phi(\vec{s}' \to \vec{s})$ is a scattering phase function of radiation transfer from entering direction $\vec{s}'$ to scattering direction $\vec{s}$.

It is obvious that angular direction $\vec{s}$ and spatial position $\vec{r}$ both affect radiant intensity I. The definition of the boundary conditions in equation (4) is necessary for the solution of equation (3). A participating medium's ability to scatter radiation energy is described by the scattering phase function Φ in RTE. There are two types of scattering: anisotropic scattering and isotropic scattering. Anisotropic scattering can scatter more energy in either a forward or a backward direction than isotropic scattering, which scatters energy equally in all directions[35].This equation gives a variation of radiation intensity in a medium given the medium temperature and boundary conditions for intensity. The outgoing intensity at wall, which is the boundary condition of equation (3), can be written as sum of the emitted and reflected ones for a diffusely emitting and reflecting wall with temperature T_w. Certain boundary constraints are applied in order to solve the RTE. Any confined opaque surface emits radiation energy through surface temperature-induced emission as well as by reflection of incoming intensity off of flame or other parts of furnace wall. This can be written as,

$$I(\vec{r}_w, \vec{s}) = \varepsilon_w I_{bw}(\vec{r}_w) + \frac{1-\varepsilon_w}{\pi}\int_{\vec{s}\cdot\vec{n}_w<0} I(\vec{r}_w, \vec{s}) \, |\vec{s}\cdot\vec{n}_w| d\Omega' \text{ for } \vec{s}\cdot\vec{n}_w > 0 \qquad (4)$$

Where, ε_w and $I_{bw} = \frac{\sigma T_w^4}{\pi}$ are emissivity and blackbody intensity of wall.

The longitudinal furnace gas and wall temperature are the foundation of this reheating furnace concept. By using the control angle and control volume formulation to solve RTE, it is able to forecast the radiation heat flux on slab surfaces [36][37][38][15]. In order to estimate the temperature distribution inside slab, the radiative heat flow is then employed as a boundary condition for heat conduction equation of slab surfaces, which is solved using a finite volume approach[14]. Unsteady components are addressed implicitly in this method of solution, whereas diffusion terms are managed by central difference scheme. The TDMA is then used to solve resulting discretized solution iteratively until steel slabs' temperature field satisfies the subsequent convergence criterion [22].

$$max\left(\frac{\left|T_{i,j}^{n}-T_{i,j}^{n-1}\right|}{T_{i,j}^{n}}\right) \leq 10^{-6} \tag{5}$$

The total radiative heat flux can be calculated by including convective heat transfer, as,

$$q_{slab}^{T} = q_{slab}^{C} + q_{slab}^{R} \tag{6}$$

Where superscript C and R represent corresponding convective and radiative heat flux By utilising the following equation, one may estimate the convective heat transfer in a reheating furnace due to flow field of hot combustible gases in the furnace enclosure,

$$q_{slab}^{C} = H_c\left(T_g - T_{slab}\right) \tag{7}$$

where, H_c is the overall heat transfer coefficient for gas and can be calculated using the relation provided by Lebedev and Sokolov [39][40].

$$H_c = 0.175\left(\frac{\dot{m}D_{eq}}{A\mu}\right)^{0.75}\left(\frac{k}{D_{eq}}\right) \tag{8}$$

According to some literature, the heat transfer coefficient of a steel slab surface is 7.8 W/m², where D_{eq}, μ, k, and A are equivalent diameter, viscosity, conductivity of gas and surface area[26]. The distribution of surface temperature of the steel slab is necessary for the continuous computation of the heat fluxes q_{slab}^{C} and q_{slab}^{R}. The 3D heat transfer conduction equation must be solved in order to calculate steel slab surface temperature continually. As boundary conditions on the surfaces of the steel slab, heat fluxes are necessary. As a result, the reheating furnace's calculation of radiation heat transfer and the resolution of the heat conduction equation in steel slabs are related. Therefore, iterative problem solving is required for the radiative heat transfer in furnace enclosure and conduction heat transfer within steel slabs.

- **Solution Method for Mathematical Model:** Both the angular direction dependency and the spectrum reliance must be taken into account in radiation transfer models. Therefore, it is necessary to determine radiation intensities in both the angular and the spatial domains. Division of angular space into $N_\theta \times N_\phi$ control angles that are evenly spaced $\Delta\theta$ and $\Delta\phi$ is the simplest way for angular discretization. To accurately reflect the physics of the issue, one can change the magnitude of these control angles.
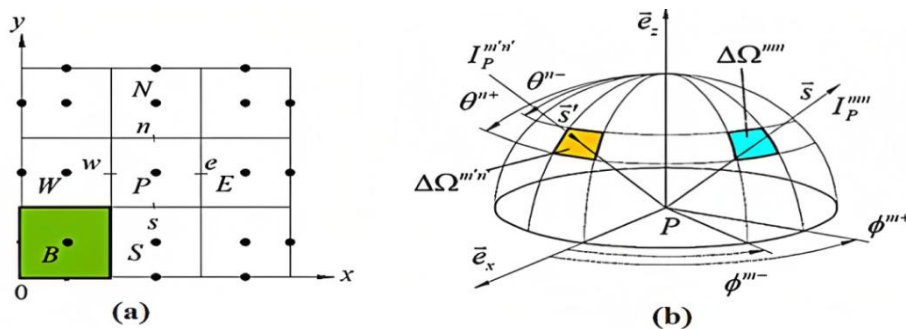
Figure 5: (a) Spatial control volume and (b) Spatial control (solid) angle.

The RTE "equation (3)" needs to be analysed in order to calculate the radiation flux on slab surface $\vec{r}_w$ (equation 2), to be used as boundary condition for equation (1). The FVM for radiation was suggested by Chui and Raithby [9], and further developed by Chai et al. [10] and Baeket al. [11] is adopted to discretize RTE. The RTE is integrated over control volume, ΔV and control angle $\Delta\Omega^m$ (see figure 5a and figure5b) to derive the final discretised equation. The following equation can be constructed by assuming that the constant magnitude of intensity inside spatial domains while permitting change in direction.

$$a_P^m I_P^m = a_E^m I_E^m + a_W^m I_W^m + a_N^m I_N^m + a_S^m I_S^m + b_P^m \qquad (9)$$

$$a_I^m = max(-\Delta A_i D_i^m, 0) \qquad (10)$$

$$a_I^m = \sum_{i=e,w,n,s} max(-\Delta A_i D_i^m, 0) + \beta_{0,P} \Delta V \Delta\Omega^m \qquad (11)$$

$$b_P^m = (S_R^m)_P \Delta V \Delta\Omega^m \qquad (12)$$

$$S_R^m = \kappa_a I_b + \frac{\sigma_s}{4\pi} \int_{\Omega'=4\pi} I^{m'} \Phi^{m' \to m} \Delta\Omega^{m'} \qquad (13)$$

$$D_i^m = \int_{\Delta\Omega^m} (\vec{s} \cdot \vec{n}_i) \, d\Omega^m \qquad (14)$$

Where D_i^m and $\vec{n}_i$ are surface area and outward unit normal vector at surface$i$ respectively. Additionally, subscript I represents E, W, N and S, while$i$represents$e$, w, n and s.

Baek et al.'s [11] description of the discretization process and associated quantities is simple to understand. The blocked-off method recommended by Chai et al. [10] can be used if radiatively inactive parts, such as the slab in furnace and the block in bottom furnace wall, exist inside the solution domain, point B (figure 5a). Even though the entire domain is included in the calculation, this approach only considers the solutions in the active regions. An additional source term is added to equation (6) in the manner described below in order to explain blocked-off treatment:

$$S^A = S_C^A + S_P^A I_P^m \qquad (15)$$

Both S_C^A and $S_P^A$are set equal to zero and LN (where LN is a huge number such as 10^{21}) respectively for a cell in inactive region. However, both S_C^A and $S_P^A$are set equal to zero in the active region. For a direct contact between an active cell and an inactive cell, such as, for point W, following conditions are applied:

$$S_C^A = -\frac{\Delta A_W D_W^m}{\Delta V \Delta\Omega^m}\left(\varepsilon_W I_{bW} + \frac{1-\varepsilon_W}{\pi} \sum_{m=1}^M I_W^m |D_W^m| \Delta\Omega^m\right) \qquad (16)$$

$$S_P^A = 0 \qquad (17)$$

At last, the coefficient of equation 8 and equation 9 are updated such that

$$a_P^m = \sum_{i=e,w,n,s} max(\Delta A_i D_i^m, 0) + (\beta_{0,P} - S_P^A)\Delta V \Delta\Omega^m \qquad (18)$$

$$b_P^m = (S_R^m + S_C^A)_P \Delta V \Delta \Omega^m \tag{19}$$

The iterative solution ends when following convergence criteria is achieved,

$$max \left(\left| \frac{I_P^m - I_P^{m,old}}{I_P^m} \right| \right) \leq 10^{-6} \tag{20}$$

Where, $I_P^{m,old}$ is the old iteration value of I_P^m. After obtaining intensity field, directional weights D_W^m can be used to estimate radiative flux on slab surface in equation (2) as,

$$q_{slab}^R = \int_{\Omega=4\pi} I(\vec{r}_w, \vec{s}) |\vec{s}.\vec{r}_w| d\Omega = \sum_{m=1}^{M} I_W^m D_W^m \tag{21}$$

The computation initialises with thermal radiation inside furnace chamber to provide radiation heat flux on each slab surface so as to obtain the specific slab temperature each time; following, heat conduction within each slab is simulated sequentially from first slab to last slab. Up until the slab is moved by a WB furnace to the following fixed beam, this computation loop is repeated. The starting slab temperature of a previously determined one at that position is used in the aforementioned calculation technique. When the slab has been in the furnace for the designated amount of time, the calculating process is over.

- **Solution Algorithm of Radiation Transfer Equation:** The radiation intensities serve as the unknowns in a series of algebraic equations produced by the FVM discretization. The resulting set of equations are solved iteratively with each time step. The collection of equations can be effectively solved using a marching order. Figure 6 depicts a potential marching sequence for Cartesian grid issues for a control angle pointing in the first quadrant. Extensions to the other three quadrants are simple and are left for interested readers to investigate. The program's structure for resolving radiation heat transfer issues is detailed in the RAT user handbook [41]. For completeness, the solution process for the scenario shown in figure 6 is outlined below.

  - For the entire domain, specify the initial intensity distribution.
  - Step up the time step to $t + \Delta t$
  - Set the guessed values to the initial or most recent nodal intensities.
  - For the scenario shown in figure 6, update the "upstream" border intensities (left and bottom walls).
  - Nodal intensities for all internal control volumes are calculated in the marching order shown in figure 6.
  - Determine how much radiation enters and leaves the right and top walls.
  - Up to convergence, go back to step 4 and redo the computations.
  - When the appropriate time has passed, stop or proceed to step 2 to move on to the next time step.
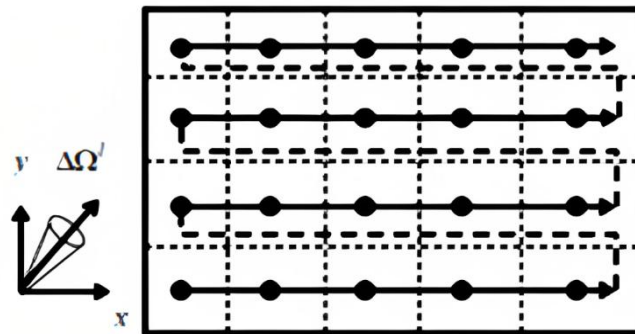
Figure 6: A possible marching order.

3. **Modelling the High Temperature Oxidation of Slabs:** Different combustion reactions, such as oxy-fuel combustion through a number of burners, are used to heat the industrial grade reheating furnace. Therefore, highly high combustible gases with temperatures between 1000°C and 1450°C, such as CO_2, H_2O (g), O_2, and N_2, are used to feed the furnace. Due to the high spectrum properties of the combustion products, such as CO_2 and H_2O (g), radiative heat transfer occurs. Hot oxidising combustion products after combustion fill the reheating furnace and oxidise the steel slabs because of their potent oxidising power at high temperatures. Slabs commonly come into contact with combustible gases in an atmosphere with such high temperatures. A number of events take place during these interactions, including initial oxygen adsorption on steel slab surfaces, chemical reaction to generate surface oxide, oxide nucleation, and subsequently growth of continuous oxide. A hollow, microcrack, or porous film is generated at the end of the process.

In order for Wustite ($Fe_{0.93}O$), Magnetite (Fe_3O_4), and Hematite (Fe_2O_3) to create three successively distinct oxide layers, oxygen must be transported through the pores in order for the process to continue. In the Ellingham/Richardson figure [55], this is demonstrated. The percentage compositions of the aforementioned three oxides, at 600°C, as stated in the literature is 96%, 4%, and 1%, respectively [56][57]. Table 4 provides Wustite's thermal characteristics by Torres and Colas [58].

Table 4: Thermophysical Characteristics of Wustite ($Fe_{0.93}O$)[28]

Wustite	Thermal Conductivity ($Wm^{-1}K^{-1}$)	Specific Heat Capacity ($Jkg^{-1}K^{-1}$)	Volumetric Density (kgm^{-3})
$Fe_{0.93}O$	3.19	724.88	7750.41

Due to Wustite's extremely low thermal conductivity in comparison to slabs, it is predicted that its presence on slab surfaces will have an impact on how heat transfers. At high temperatures, the rate of oxide scale formation on steel slab surfaces often follows a parabolic regime. The thickness of the scale can be expressed as

$$x^2 = k_p t \tag{22}$$

Where, x, t are oxide thickness and oxidation period respectively, and parabolic rate constant, k_p, is exponentially dependent on temperature as,

$$k_p = k_o e^{-\frac{Q}{RT}} \qquad (23)$$

where, T, R and Qare temperature (in kelvin), gas constant, and the activation energy of the iron oxidation. Numerous researchers use the following expression for the parabolic rate constant [12]:

$$k_p = 6.1 e^{-\frac{169,452}{RT}} \qquad (24)$$

IV. MATHEMATICAL MODELLING OF REHEATING FURNACE

1. **Transient Heating Characteristics of Slabs/Billets in Reheating Furnace:** Kim evaluated the thermal behaviour and heat transfer properties of the slab using different parameters, such as the slab's emissivity and absorption coefficient [22]. The temperature distribution in the furnace enclosure's slabs is depicted in figure 7 (a). The five zones of a WB furnace are charging, preheating, heating and soaking zones. Slabs are charged into furnace from the non-firing zone. The slab's charging temperature is 21.2°C, and as it comes into contact with hot combustible gases, that temperature rises. The slab's right corner section has the highest non-firing zone temperature of 346.1°C. It helps to maintain the slab's uniform temperature profile and lessens the temperature gradient within slab as slabs proceed to the following successive zones, where the temperature rises to 1150°C in the heating zone and drops to 90°C in the soaking zone. The radiation behaviour in the furnace chamber is shown in figure7(b). As we can see, initially, the heat flux vectors are relatively more concentrated in no firing zone and charging zone due to large temperature difference between slabs and furnace gases. Thereafter, the concentration of the heat flux vector decreases. Due to the hot slab's higher temperature compared to the soaking zone gas temperature, radiative heat flux from the slab is released into the soaking zone. Consequently, the slab's temperature was more evenly distributed [22].Figure 8 shows that the first slab has a significant temperature difference from the furnace side, which causes radiation flux at one end of the slab. Depending on the temperature difference between the furnace zone and the slab, it may rise or fall.
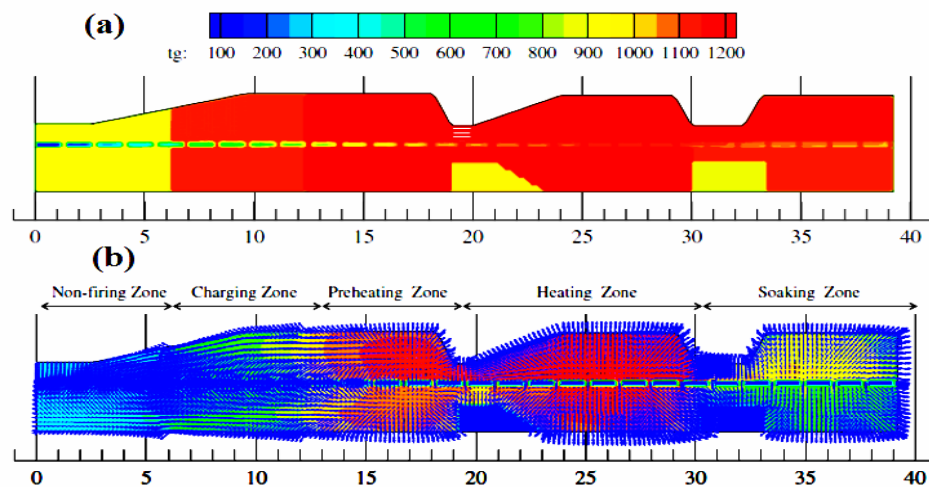
Figure 7: (a) Temperature Distribution (°C), and (b) Radiation flux vectors in furnace enclosure[22].
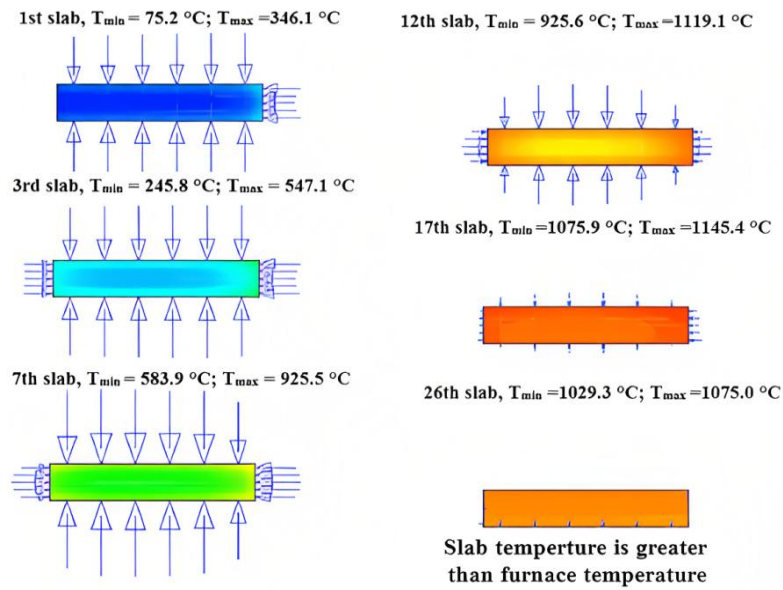
**Figure 8:** Radiation flux vectors on slab surface and temperature contours within slab [22].

2. **Influence of Fuel Feeding Rate on the Furnace Enclosure's Interior Heating Profile:** Table 5 displays the methods that Han et al. used to evaluate the heating behaviour of the slab in a reheating furnace at varied fuel feed proportions. Fuel is supplied into the furnace at the same rate in each of these scenarios (22,320 m3/h), but the rates for the upper and lower zones are set at 44.9% and 54.98%, respectively. Because heat is lost through the skid support system, the fuel feed rate is higher in lower zone [24].

Table 5: Fuel Feeding Settings of Lower Zone and Upper Zone in Reheating Furnace, m³/h (%) [24]

Case	Lower zone			Upper zone		
	Pre-heating	**Heating**	**Soaking**	**Pre-heating**	**Heating**	**Soaking**
1	4221.1 (33.4)	4221.1 (33.4)	4221.1 (33.4)	3521.1 (33.4)	3521.1 (33.4)	3521.1 (33.4)
2	5111.1 (40.1)	4471.1 (35.1)	3191.1 (25.1)	4181.1 (40.1)	3661.1 (35.1)	2611.1 (25.1)
3	5111.1 (40.1)	5112.1 (40.1)	2561.1 (20.1)	4181.1 (40.1)	4181.1 (40.1)	2081.1 (20.1)
4	5736.1 (45.1)	5116.1 (40.1)	1921.1 (15.1)	4706.1 (15.1)	4176.1 (40.1)	1571.1 (15.1)
5	6381.1 (50.1)	4471.1 (35.1)	1921.1 (15.1)	5221.1 (50.1)	3661.1 (35.1)	1571.1 (15.1)
6	7021.1 (55.1)	3831.1 (30.1)	1921.1 (15.1)	5751.1 (55.1)	3131.1 (30.1)	1571.1 (15.1)
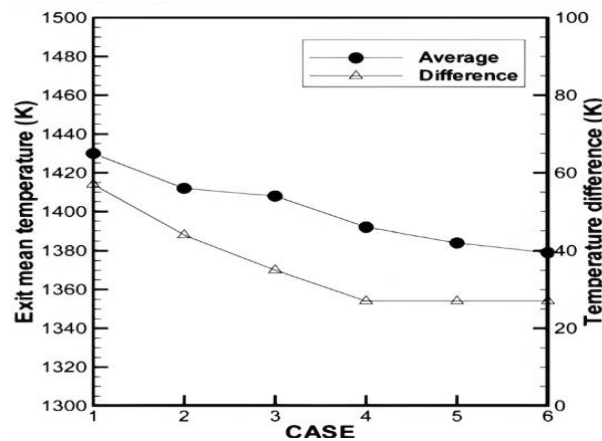
Figure 9: Slab mean temperature and temperature variation at exit for various fuel feeding rate (m^3/h) [24]
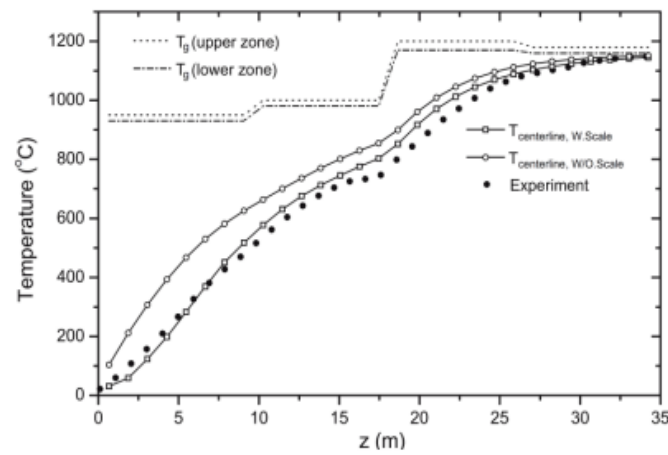
According to figure 9, the temperature differential between the slab in both parts of the furnace increases when the percentage of fuel feed rate is at its highest in soaking zone (Cases 1, 2, and 3). In this situation, slab gets heated more. However, when less fuel is fed into the soaking zone (cases 4, 5, and 6), temperature uniformity of slabs increases. In soaking zone, the temperature differential within slab reduces, and slab's mean temperature follows a similar trend. obtained the ideal thermal profile of the slabs at furnace's output, and the findings showed that constrained fuel input rate provides slabs of high quality. It has been noted that total heat balances are used to determine the combustible gases and wall's unknown temperatures.

3. **Scale Growth on Top and Bottom Surfaces of Slab:** In order to forecast the development of scale on slab surface in the longitudinal direction of the gas temperature and its impact on the slabs' heat transfer characteristics and temperature profile, Jang et al. have built a model for the WB furnace. Additionally, they looked into the temperature variationon the slab surface, with or without scale, as well as the heat flux that impinges on slab surface. When a furnace was loaded with hot combustible gases and modelled as a radiating medium with spatially variable temperature. Due to their extremely high spectral radiative qualities, these hot gases are utilised as a radiation media inside the furnace enclosure. Depending on the temperature, the slab's thermo-physical characteristics change.

However, the temperature and distribution of combustible gas concentrations in the furnace enclosure varies depending on the flow and combustion at different locations[28]. Due to the oxidation behaviour of gases, these combustible gases oxidise the slab surface at very high temperatures. Metals can react with hot gases as a result of oxygen absorption on slab surfaces, chemical reactions that result in the formation of surface oxide or oxide nucleation, and finally the creation of a continuous oxide coating. The film shows several cracks and micro-porosity as well.

Table 6: Thermophysical Properties of Steel Slab [28]

| Temperature (°C)	Thermal Conductivity (W/m K)	Specific Heat Capacity (J/kg K)	Volumetric Density (kg/m³)
30.0	26.87	299.01	
400.0	25.45	401.62	
600.0	22.71	512.01	7779.0
800.0	20.88	542.83	
1000.0	23.79	478.94	

Figure 10: Both anticipated and experimental data for longitudinal temperature profile of slab's centreline temperature, with and without scale[28].

According to figure 10, the temperature of scale-free slab is more than the temperature in the middle of the scale-covered slab, and the anticipated temperature profile of the scale-free slab fits well with the outcome of scale-covered slab. The temperature difference at furnace's outflow progressively drops to 10°C as the slab heats up, as seen in the image. When results are compared to experimental data, results that take scale effect into account are in a greater agreement than results that do not. This means that in order to more precisely analyse the thermal behaviour of the slab in reheating furnace, scale formation and growth are one of the significant elements that must be taken into account. The slabs are heated by hot, oxidising combustion fumes that are emitted from the reheating furnace. Additionally, these gases interact with the steel slabs, forming an iron oxide coating that eventually transforms into scale. As was already established, the majority of metals exhibit a parabolic regime for scale growth at high temperatures.
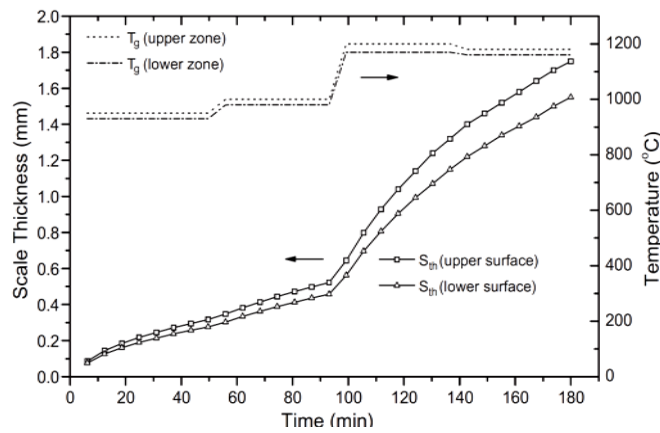
Figure 11: Growth of iron oxide scale on slab's top and bottom surfaces in the WB furnace[28]

4. **Effect of Slab Scaling on Heat Flux in WB Furnace:** The accompanying illustration shows how heat flux is distributed over the slab. As can be seen, in the firing zone, heat flux is higher on top than the bottom of slabs. Additionally, heat flux vector should vanish as we observe in the soaking zone when the temperature differential between the slab surfaces and furnace walls reduces. Reverse heat flux is seen in the soaking zone because relatively little heat is released from the slabs in this area. The reason why slab temperature is higher in soaking zone than furnace enclosure is due to the fact that the heating zone temperature is higher than the temperature of the soaking zone [28].In contrast to a steel slab, scale has a much lower thermal conductivity, while its specific heat is somewhat higher. Due to scale's poor thermal conductivity, it prevents heat from transferring from hot furnace gases and walls to the steel slab, which has a substantial impact on the slab's heat transfer characteristics. In addition, scale tends to heat itself slowly due to its high specific heat, which lowers the rate of heat transfer to a slab when it is surrounded by scale compared to case of no scale formation [31].
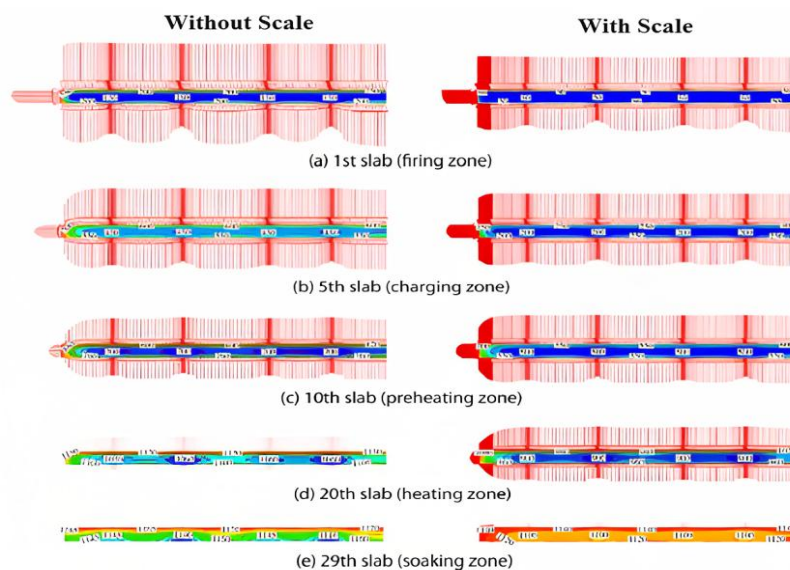
Figure 12: Heat flux variation on slab surface and temperature variation within slab scale in furnace zones[28]

In order to determine the radiative heat transfer within the furnace and conductive heat transfer inside billets using the FVM, Harish and Dutta developed a mathematical approach. Additionally, they used correlation to predict the convective heat flux on the surface of billets (equation 42). However, by adding another component to two-dimensional heat conduction equations, the motion of billets in pusher-type reheat furnaces and the temperature variation inside the billets can be represented using equation 43 [26].

$$\rho C_p \frac{\partial T}{\partial t} = \frac{\partial}{\partial x}\left(k \frac{\partial T}{\partial x}\right) + \frac{\partial}{\partial y}\left(k \frac{\partial T}{\partial y}\right) \tag{42}$$

$$\rho C_p \frac{\partial T}{\partial t} = \frac{\partial}{\partial x}\left(k \frac{\partial T}{\partial x}\right) + \frac{\partial}{\partial y}\left(k \frac{\partial T}{\partial y}\right) - \rho C_p u \frac{\partial T}{\partial x} \tag{43}$$

In order to solve this equation, a heat flow boundary condition is required, and the radiation and convection modes of heat transmission directly expose the billets.

$$-k \left[\frac{\partial T}{\partial x}\right]_{surface} = q_r + q_c \tag{44}$$

According to published studies, radiation accounts for 90% of all heat transfer, with the remaining 10% occurring by convective heat transfer when combustible furnace gases are present. It is necessary to take into account heat transport as well as numerically solve the equations (using FVM) to get results as a temperature distribution within the billets inside the reheat furnace. Additionally, a conventional correlation is employed to describe the convective heat flux term and calculate convective heat flow.

$$q_c = h(T - T_\infty) \tag{45}$$

where T is the temperature of the gaseous layer just next to the billet, and h and T_∞ are convection heat transfer coefficient and surface temperature of billet at any specified point, respectively. Using the Lebedev and Sokolov relation, *h* for a surface exposed to combustion gases is taken into consideration [39].

$$h = 0.175 \left(\frac{\dot{m} D_{eq}}{A \mu}\right)^{0.75} \left(\frac{k}{D_{eq}}\right) \tag{46}$$

where, D_{eq}, A, μ and k are equivalent diameter, roof surface area, viscosity and conductivity of the gas respectively.

5. Influence of Billet Thickness on Centreline Temperature Profile: As seen in figure 13, the centreline temperature of billet is also influenced by its thickness[26]. The amount of time billets spend in furnace rises with increasing billet size. Thus, the cross-sectional area of billets determines the ideal residence duration and the intensity of heating in order to achieve the uniform temperature profile.
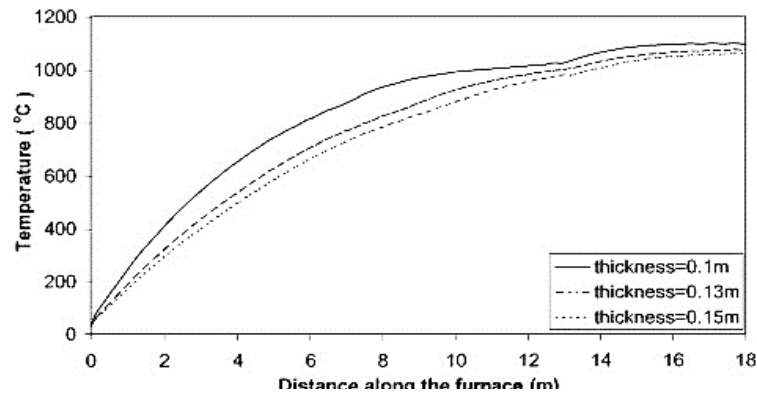
Figure 13: Centreline temperature profile for billets in furnace for various thickness[26]

6. **Estimation of Skid Mark Formation in Reheating Furnace:** A solution to the transient conduction equation in a radiative furnace was put out by Jang et al. They discovered that the primary source of the heat flux impinging on slab surface is thermal radiation from the reheating furnace. Additionally, they demonstrated that the effect of the slab's emissivity on the temperature variation of slab is greater than that of furnace wall's emissivity since the slab is heated primarily by combustion gases inside the furnace[27].Researchers have examined the skid mark effect on slabs by varying the residence time and emissivity of the slabs, and they have discovered that 180 minutes is the ideal residence time.

Additionally, as the slab is heated mostly by furnace gas rather than the furnace wall, a very modest effect of the emissivity of the furnace wall is seen in the temperature profile of the slab [20]. As seen in figure 14, the shielding action of the skids causes a heat flow to be lowered around the slab in the skid contact zone. As a result, the temperature in this area of the surface is relatively low, which could alter how hot or cold the slabs' lower and upper sides are.
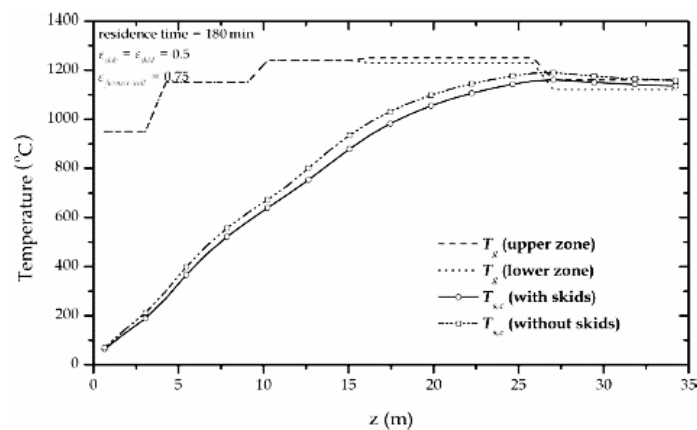

Figure 14: Slab centreline temperature profile in a longitudinal direction, with and without skids [27]
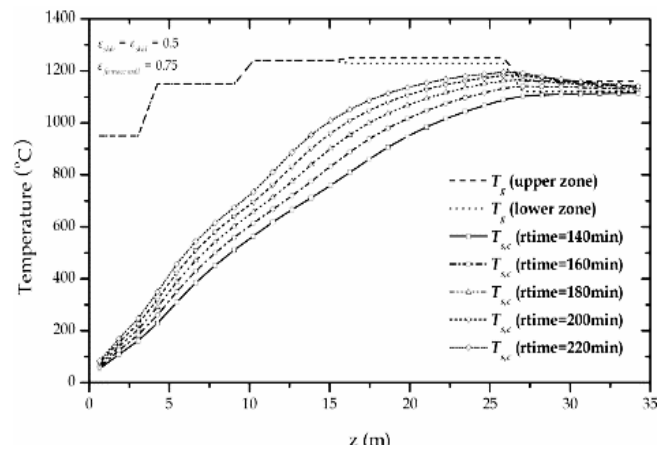
**Figure 15:** Effect of residence time on slab temperature profile in longitudinal direction of a WB furnace[27]

7. **Influence of Residence Time on Heating Characteristics of Slabs/Billets:** The length of time the furnace is in use directly affects how quickly it produces heat, how quickly it consumes energy, and how quickly it emits pollutants. Finding the ideal residence time is crucial for the reheat furnace to operate well and economically. Figure 16 shows that temperature rises with residence time but has minute effect on the temperature in the soaking zone at the furnace outflow and is practically the same after 3 hours. [27].The optimal residence duration, uniform temperature distribution, and skid mark effect on the slab were all predicted by Lee using a mathematical model that also determined the temperature profile of the slab at its centre and top surface [22]. As can be observed from figure16, the anticipated centreline and upper surface temperatures of slab and the simulated outcomes are in conformation. The difference between projected and actual temperatures of slab surface at the end of furnace is 1%, and the centreline is within 0.5% of that difference.
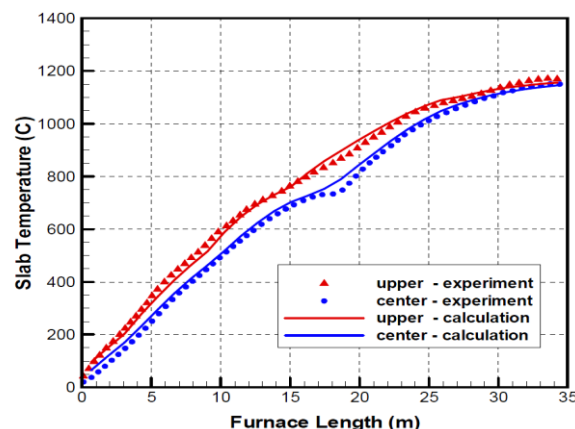
Figure 16: Assessment of anticipated and experimental temperature profile of slab [29]

By changing the furnace temperature by around 20°C from the standard pattern, the heating performance of the slab is improved. The slab temperature has been seen to be more evenly spread, and the best residence time was found to be at the new pattern of furnace temperature, which has a minimum skid mark of 34°C [22]. In addition, Lee et.

al. created a model for two alternative charging temperatures and found that the differential in surface and centre temperature, and the slab exit temperature all steadily diminish over the course of residence time [23]. Additionally, it has been noted that hot charging results in less skid marks and temperature differences between the slab's surface and middle than cold charging does.
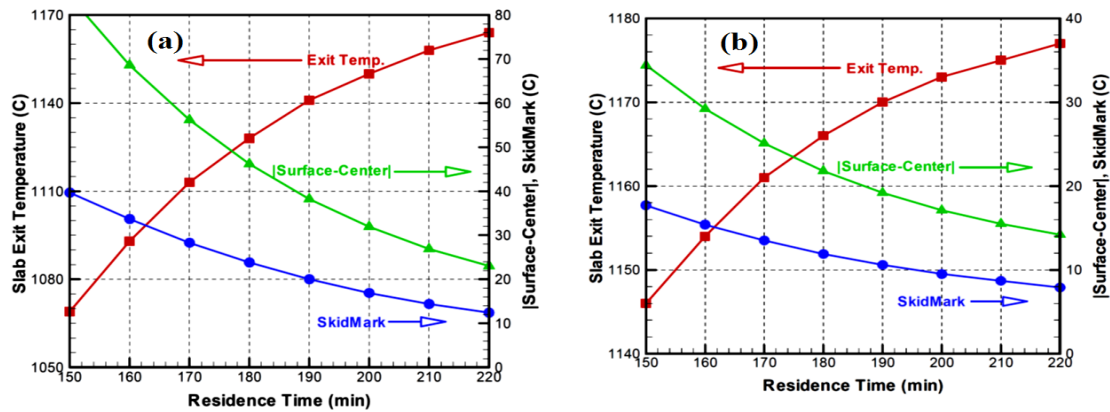
**Figure 17:** Heating characteristics with residence time for hot charging (a) Cold charging (b) HCR [30]

The techniques were created by Han et al. to determine the ideal residence time that satisfied the goal temperature. The model they used to simulate the combustion gases inside the furnace was WSGGM. This model is more accurate than the grey gas model because it provides a better estimate of gas radiation by using the block-off technique to tackle inactive regions like slabs and dead zones and prevent the use of meaningless intensity [16]. The goal slab temperature in this literature is 1273 K, and the maximum slab temperature variance is 50 K. As can be shown in figure18, this condition is produced by two examples with residence times of 5568 and 6496 seconds. The goal slab temperature ought to be the slab's optimal mean temperature. The example of 6960 seconds satisfies the requirement for a temperature difference from the 28th slab and obtains a temperature that is close to the desired one.
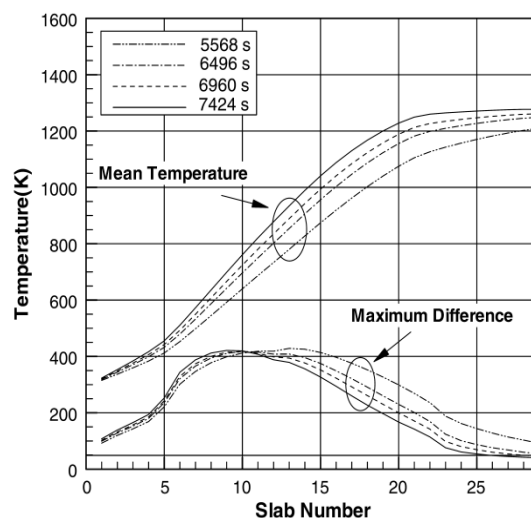
Figure 18: Impact of the four distinct residence times on the slab's mean temperature [23]

The top surface profile of billet is shown in figure19 changing in accordance with the speed of the moving slab, which is directly connected to residence period of the furnace. The transverse movement speed of the billet affects residence time. While all other parameters remained the same, effect on a $0.1312m^2$ billet was determined for velocities: 0.003 m/s, 0.002 m/s, and 0.001 m/s. The computed residence times were 6000.0 s, 9000.0 s, and 18000.0 s, respectively.

As can be seen in figure19, the top surface temperature is influenced by the billet's motion. As heat cannot disperse inside the billets in such a short period of time, the temperature distribution throughout the furnace is prevented if the billets move more quickly. The upper surface temperature and temperature variation of the billets are reached, which is required for ideal conditions, as the residence duration of the furnace grows owing to the reduced speed of the billet, as can be seen in figure Additionally, it causes the thermal stress that is produced within the billets as a result of uneven heating to decrease. By taking into account the radiation heat exchange inside furnace and convection heat transfer, with combustion gases being inserted as a boundary condition, G.W. Lee and his co-worker also constructed a model to produce radiation flux. They discovered that a slab can be heated with more emissivity and residence duration [25].
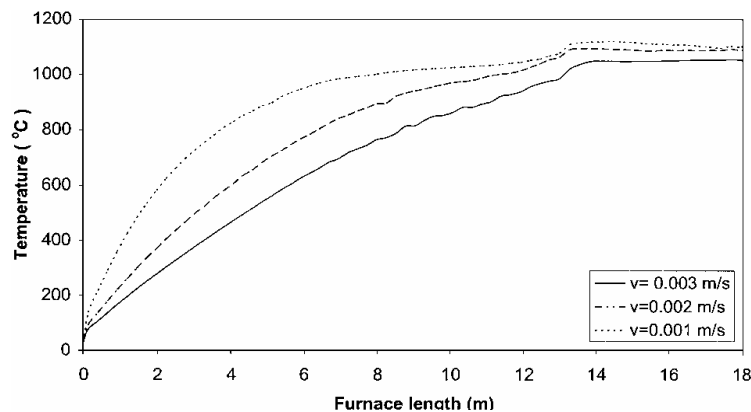
Figure 19: Impact of different traverse speeds on the top surface temperature profile of billets [26]

The behaviour of the radiation flux over the slabs at four residence times is depicted in figure 20. It was found that while the initial radiation flux grows significantly over the entire residence duration, the rate of heating changes afterwards due to the variable heat flux. Because increased residence time encouraged more uniform temperature distribution in slabs at the end zone of the furnace, slabs with high residence time that correlate to very low radiation flux are detected. Due to little temperature difference between slabs and the furnace zone, the radiation heat flow decreased. Han et al. discovered the consistency of the temperature within the slab at various residence times and slab numbers. Although the slab's goal temperature is 1273 K, the optimal condition was met starting from 26th slab in the case of 7425 seconds and from 28th slab in the case of 6961 seconds.
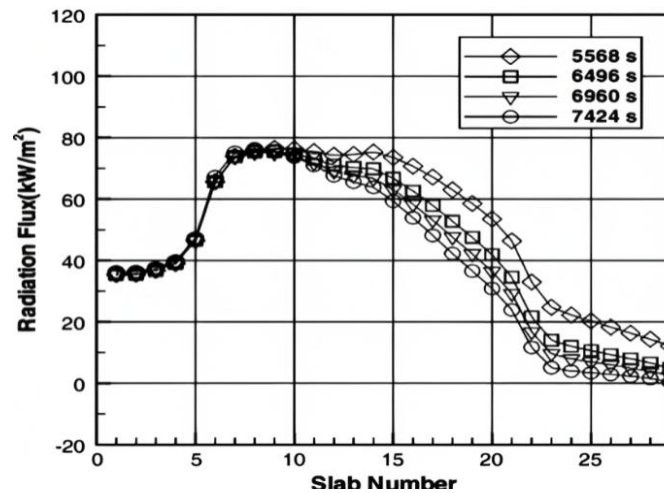
**Figure 20:** Radiative fluxes for The Various Residence Times [23]

8. **Slab Emissivity's Impact on the Slab/Billet Anticipated Temperature Profile:** With an increase in the slab's emissivity (which ranged from 0.3 to 1.0), the temperature rises. Figure 21 shows the impact of slab emissivity on temperature profile. When the surface of the slab turns black, it absorbs more heat. Keeping the furnace wall emissivity and absorption coefficient at 0.15 m^{-1} and 0.75, respectively results in slight temperature variation at the furnace zone's end [15].Three different emissivity were studied, and the results showed that as emissivity increases, so do the features of the billet temperature because more radiation is absorbed at the surface of the billet, resulting in higher temperatures for the billets. The temperature of the billet surface quickly approaches that of the gas and furnace roof at high emissivity.
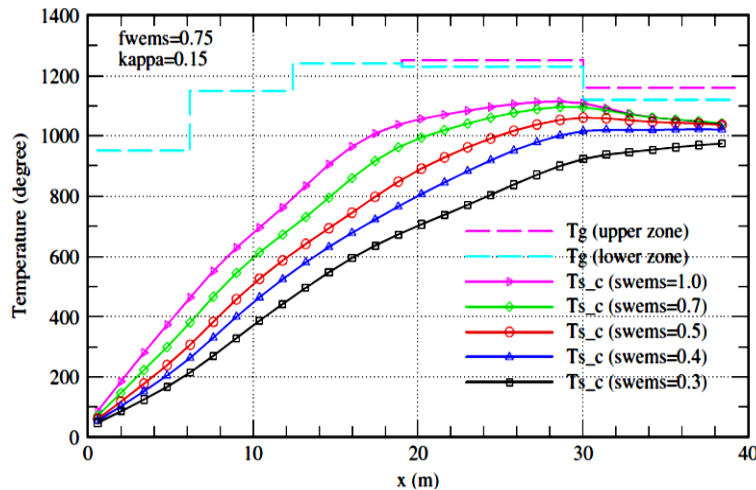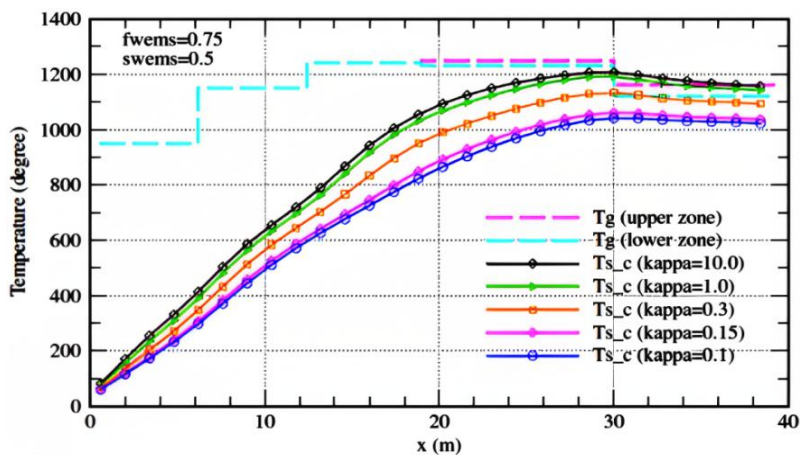

Figure 21: Influence of the slab's emissivity on the slab's anticipated longitudinal temperature profile[22]

9. **Impact of the Absorption Coefficient on Slab's Anticipated Longitudinal Profile:** Combustible gases like CO_2 and H_2O are the furnace's primary source of radiative heat transfer. Absorption coefficient and slab emissivity affect radiation in different ways. The impact of furnace medium's absorption coefficient on longitudinal temperature profile at

slab's centreline temperature is shown in figure 22. As the medium surrounding the slab becomes more active with an increase in absorption coefficient, the centreline temperature of the slab rises as absorption coefficient grows from 0.1 to 10 m^{-1}.
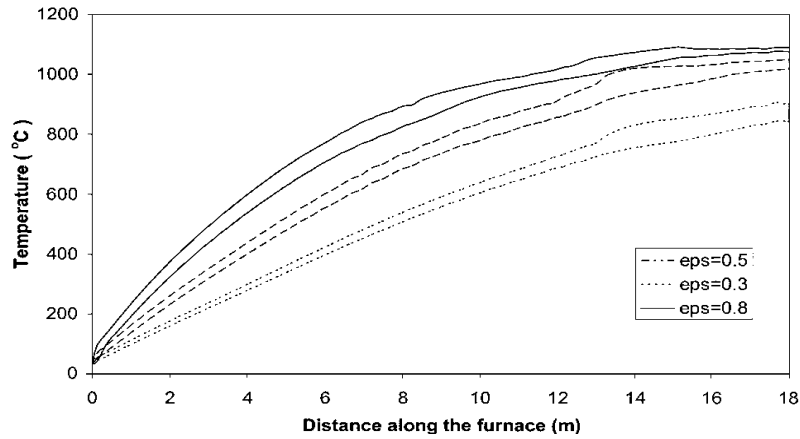
**Figure 22:** Temperature assessment of the billet's top surface and centre for varying load emissivity[26]

Figure 23: Impact of the absorption coefficient on slab's anticipated longitudinal temperature profile[22]

10. **Radiation Slab Heating Analysis for Different Fuel Gas Composition in Reheat Furnace:** In presence of combustion gases like CO_2 and H_2O, Han and Chang suggest the WSGGM model to obtain the radiation heat transfer inside the furnace. Compared to BFG, COG is more calorific dense. Therefore, a fuel fired reheating furnace's performance can be improved by using a mixing strategy with both fuel gases. To save fuel, improve furnace performance, and ensure that the slabs are heated uniformly, it is best to explore the ideal mixing criteria for two combustion gases [25].As can be seen in figure24(a), the percentage of COG grows along with the slab's heat flux. Due to its high calorific value, which raises the temperature of furnace walls, gases and flame, the proportion of COG, which determines the maximal temperature of the slabs. Due to their stronger radiative spectrum features, these combustible gases participate in radiative heat transfer at higher temperatures. The COG % also influences the temperature differential between the slabs at the same time. A higher COG percentage makes it easier to distribute

heat evenly throughout slabs. The starting temperature difference within the slabs is altered at various COG proportions, as can be observed in figure24(b). Temperature difference rises as COG percentage rises, and there is some reversion between the 19th and 24th slabs. Thereafter, temperature difference falls as COG proportion rises.
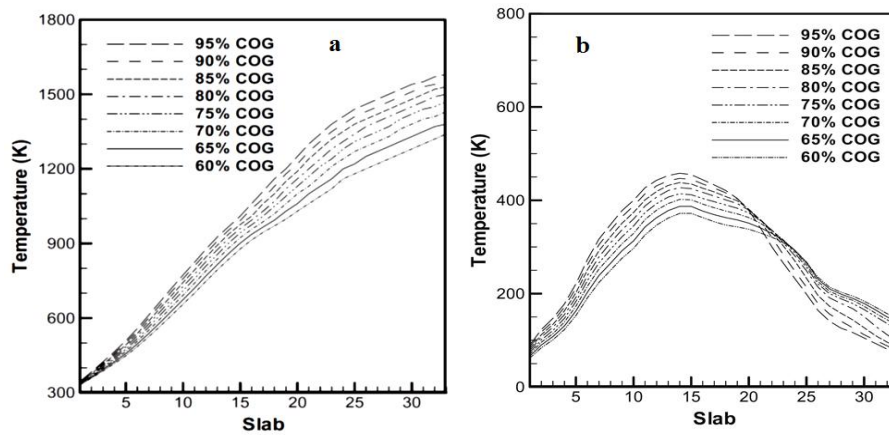

Figure 24: Slab temperature profiles for different BFG and COG mixture ratios (a) Slab Mean Temperature (b) Temperature difference of the slab[25]

By taking into account all potential paths of radiative heat transfer using WSGGM for better estimation of combustible gases radiation, a mathematical heat transfer model based on zone approaches was created by Emadi et al. to account for the heating properties of billet in a reheating furnace with a walking hearth design and 3D radiation modelling. They looked into how the emissivity of the furnace zones' walls and temperature of the billet were affected by the convection heat transfer coefficient. They also studied how emissivity affected the temperature of the billet and residence time. They found that as emissivity rose from 0.7 to 0.95, residence time decreased by up to 5%. According to their predictions, the emissivity rises in the preheating and nonfiring zones relative to the heating and soaking zones and has a greater effect on thermal behaviour [42].
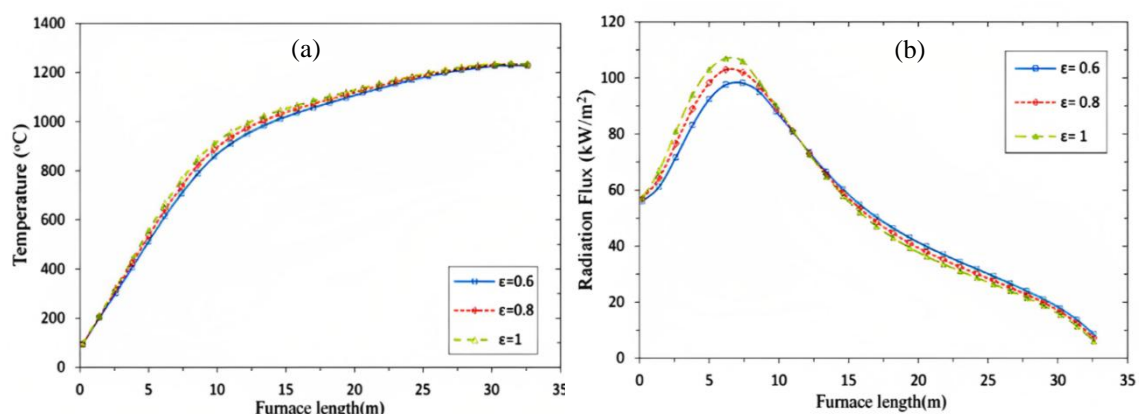
Figure 25: Variation of furnace wall emissivity on (a) temperature profile (b) radiation flux of billet surface along the reheating furnace length [42]

11. **Analysis of Slab Heating Efficiency in Walking Beam Furnace:** As radiation heat flow is independent of the COG % in the soaking zone, the highest performance of reheating furnace is reached with the lowest percentages of COG. The soaking zone has a very slight temperature differential. As a result, the radiation flux in the soaking zone at various COG percentages is nearly comparable. As can be observed in figure26, the efficiency of the reheating furnace declines as the percentage of COG rises. A lower COG percentage (60%) results in greater efficiency, but it also lengthens the time the slabs spend in the furnace. As a result, the COG % under constant fuel input conditions, which also raises slab exhaust temperature, can be increased to boost the furnace's production rate. While the reheating furnace's efficiency is only about 40%, slab emission temperature may be satisfied in the COG range of 75–80%.
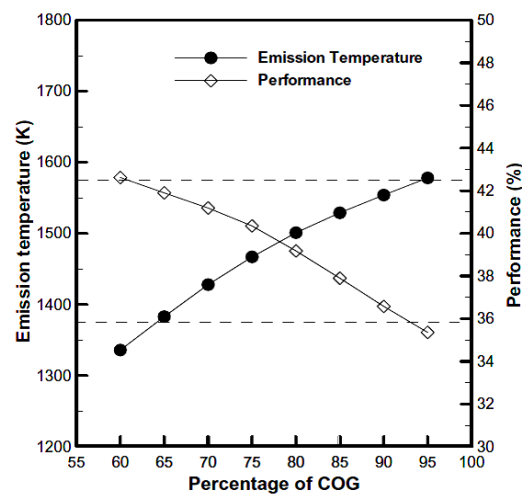
Figure 26: Influence of slab emission temperature and heating performance of reheat furnace by altering COG percentage[25].

V. CONCLUSION

After the extensive literature search, a multitude of mathematical modelling methods are being used to deal with optimization of slab residence time inside the reheating furnace and increase its overall efficiency. By finding the optimal duration for which slabs remain inside the furnace, it is possible to minimize energy consumption and maximize productivity. This, in turn, leads to significant cost savings and a more sustainable operation. These methods provide a systematic approach to understanding the complex dynamics involved in the reheating process. By utilizing mathematical equations and algorithms, researchers can simulate various scenarios and evaluate their impact on slab residence time. One such method is the utilization of optimization algorithms. These algorithms enable researchers to identify the optimal combination of parameters that result in the desired slab residence time. Further, numerical modelling when coupled with user defined function (UDF) can give highly precise results, thus making it one of the economical and time intensive method other than online simulation methods. Further research can be done based on numerical modelling to reduce the computational cost and developing novel methods to optimize the slab residence time meanwhile increasing the efficiency of reheating furnaces.

REFERENCES

[1] S. G. Jansto, "Reheat furnace operational parameters affecting hot roll quality of microalloyed long products," 2015.

[2] D. R. Kreuzer, A. Werner, and D. R. K. A. Werner, "Implementation of Models for reheating processes in industrial furnaces," pp. 376–387, 2011, doi: 10.3384/ecp11063376.

[3] W. Trinks, "Industrial furnaces," *J. Franklin Inst.*, vol. 254, no. 2, p. 186, Aug. 1952, doi: 10.1016/0016-0032(52)90645-5.

[4] P. K. Thakur, S. K. Prakash, K. G. Murlidharan, and S. S. Das, "A review on efficient energy optimization in reheating furnaces," no. December, pp. 43–49, 2014.

[5] U. Nations and I. Development, "IRON & STEEL INDUSTRY," 1992.

[6] P. Marino, a. Pignotti, and D. Solis, "Control of pusher furnaces for steel slab reheating using a numerical model," *Lat. Am. Appl. Res.*, vol. 34, no. 4, pp. 249–255, 2004.

[7] T. Morgado, P. J. Coelho, and P. Talukdar, "Assessment of uniform temperature assumption in zoning on the numerical simulation of a walking beam reheating furnace," *Appl. Therm. Eng.*, vol. 76, pp. 496–508, 2015, doi: 10.1016/j.applthermaleng.2014.11.054.

[8] M. F. Modest, "The Weighted-Sum-of-Gray-Gases Model for Arbitrary Solution Methods in Radiative Transfer," *J. Heat Transfer*, vol. 113, no. 3, p. 650, 1991, doi: 10.1115/1.2910614.

[9] A. Jaklič, F. Vode, and T. Kolenko, "Online simulation model of the slab-reheating process in a pusher-type furnace," *Appl. Therm. Eng.*, vol. 27, no. 5–6, pp. 1105–1114, 2007, doi: 10.1016/j.applthermaleng.2006.07.033.

[10] M. Zajemska, A. Poskart, M. Zajemska, and A. Poskart, "Modellazione Prediction of the chemical composition of combustion products in metallurgical reheating furnaces by use of numerical methods Memorie," pp. 33–40.

[11] P. Kumar, "Training Manual on Energy Efficiency for Small and Medium Enterprises," 2010. [Online]. Available: http://www.apo-tokyo.org/00e-books/GP-21_TMEE/GP-21_TMEE.pdf

[12] R. Y. Chen and W. Y. D. Yuen, "Review of the high-temperature oxidation of iron and carbon steels in air or oxygen," *Oxid. Met.*, vol. 59, no. 5–6, pp. 433–468, 2003, doi: 10.1023/A:1023685905159.

[13] H. J. Karimi and M. H. Saidi, "Heat Transfer and Energy Analysis of a Pusher Type Reheating Furnace Using Oxygen Enhanced Air for Combustion," *J. Iron Steel Res. Int.*, vol. 17, no. 4, pp. 12–17, Apr. 2010, doi: http://dx.doi.org/10.1016/S1006-706X(10)60079-9.

[14] S. Patankar, "Numerical heat transfer and fluid flow," *Series in coputational methods in mechanics and thermal sciences*. pp. 1–197, 1980.

[15] S. W. Baek, M. Y. Kim, and J. S. Kim, "Nonorthogonal Finite-Volume Solutions of Radiative Heat Transfer in a Three-Dimensional Enclosure," *Numer. Heat Transf. Part B Fundam.*, vol. 34, no. 4, pp. 419–437, 1998, doi: 10.1080/10407799808915066.

[16] Y. Yang and Y. Lu, "Development of a computer control model for slab reheating furnaces," *Comput. Ind.*, vol. 7, no. 2, pp. 145–154, 1986, doi: 10.1016/0166-3615(86)90036-9.

[17] Y. Yang and Y. Lu, "Dynamic model based optimization control for reheating furnaces," *Comput. Ind.*, vol. 10, no. 1, pp. 11–20, 1988, doi: 10.1016/0166-3615(88)90044-9.

[18] J. Srisertpol, S. Tantrairatn, P. Tragrunwong, and V. Khomphis, "Estimation of the mathematical model of the reheating furnace walking hearth type in heating curve up process," *Int. J. Math. Model. Methods Appl. Sci.*, vol. 5, no. 1, pp. 167–174, 2011.

[19] J. Srisertpol and V. Khomphis, "Open-loop Identification of the Mathematical Model of the Reheating Furnace Walking Hearth Type in Manufacturing Process," vol. 23, no. Icsmo, pp. 24–30, 2012.

[20] T. Pongam, V. Khomphis, and J. Srisertpol, "System modeling and temperature control of reheating furnace walking hearth type in the setting up process," *J. Mech. Sci. Technol.*, vol. 28, no. 8, pp. 3377–3385, 2014, doi: 10.1007/s12206-014-0750-x.

[21] M. Cuim, H. G. Chen, L. Xu, and B. Wu, "Total Heat Exchange Factor Based on Non-Gray Radiation Properties of Gas in Reheating Furnace," *J. Iron Steel Res. Int.*, vol. 16, no. 3, pp. 27–31, 2009, doi: 10.1016/S1006-706X(09)60039-X.

[22] M. Y. Kim, "A heat transfer model for the analysis of transient heating of the slab in a direct-fired walking beam type reheating furnace," vol. 50, pp. 3740–3748, 2007, doi: 10.1016/j.ijheatmasstransfer.2007.02.023.

[23] S. Heon, S. Wook, and M. Young, "Transient radiative heating characteristics of slabs in a walking beam type reheating furnace," *Int. J. Heat Mass Transf.*, vol. 52, no. 3–4, pp. 1005–1011, 2009, doi: 10.1016/j.ijheatmasstransfer.2008.07.030.

[24] S. Heon, D. Chang, and C. Huh, "Efficiency analysis of radiative slab heating in a walking-beam-type

reheating furnace," *Energy*, vol. 36, no. 2, pp. 1265–1272, 2011, doi: 10.1016/j.energy.2010.11.018.

[25] S. H. Han and D. Chang, "Radiative slab heating analysis for various fuel gas compositions in an axial-fired reheating furnace," *Int. J. Heat Mass Transf.*, vol. 55, no. 15–16, pp. 4029–4036, 2012, doi: 10.1016/j.ijheatmasstransfer.2012.03.041.

[26] J. Harish and P. Dutta, "Heat transfer analysis of pusher type reheat furnace," vol. 32, no. 2, pp. 151–158, 2005, doi: 10.1179/174328105X23923.

[27] J. H. Jang, D. E. Lee, C. Kim, and M. Y. Kim, "Prediction of Furnace Heat Transfer and Its Influence on the Steel Slab Heating and Skid Mark Formation in a Reheating Furnace," vol. 48, no. 10, pp. 1325–1330, 2008.

[28] J. Hyun, D. Eun, M. Young, and H. Gon, "Investigation of the slab heating characteristics in a reheating furnace with the formation and growth of scale on the slab surface," *Int. J. Heat Mass Transf.*, vol. 53, no. 19–20, pp. 4326–4332, 2010, doi: 10.1016/j.ijheatmasstransfer.2010.05.061.

[29] D. Lee, "Evaluation of Optimal Residence Time in a Hot Rolled Reheating Furnace," pp. 1180–1183, 2011.

[30] D. E. Lee and M. Y. Kim, "Optimum residence time for steel productivity and energy saving in a hot rolled reheating furnace," vol. 27, no. 9, pp. 2869–2877, 2013, doi: 10.1007/s12206-013-0735-1.

[31] M. Y. Kim, "Effect of Scale on Slab Heat Transfer in a Walking Beam Type Reheating Furnace," vol. 7, no. 7, pp. 410–414, 2013.

[32] G. W. Lee and M. Y. Kim, "On the Thermal Behavior of the Slab in a Reheating Furnace with Radiation," vol. 8, no. 5, pp. 913–918, 2014.

[33] V. K. Singh, P. Talukdar, and P. J. Coelho, "Performance Evaluation of Two Heat Transfer Models of a Walking Beam Type Reheat Furnace," *Heat Transf. Eng.*, vol. 36, no. 1, pp. 91–101, 2015, doi: 10.1080/01457632.2014.906287.

[34] V. K. Singh and P. Talukdar, "Comparisons of different heat transfer models of a walking beam type reheat furnace," *Int. Commun. Heat Mass Transf.*, vol. 47, pp. 20–26, 2013, doi: 10.1016/j.icheatmasstransfer.2013.06.004.

[35] J. C. Chai and P. Rath, "Discrete-Ordinates and Finite-Volume Methods for Radiation Heat Transfer," *Treat. Therm. Radiat. Heat Transf. Probl.*, pp. 1–15, 2006.

[36] E. H. Chui and G. D. Raithby, "Computation of radiant heat transfer on a nonorthogonal mesh using the finite–volume method," *Numer. Heat Transf. Part B Fundam.*, vol. 23, no. 3, pp. 269–288, Apr. 1993, doi: 10.1080/10407799308914901.

[37] J. C. Chai, H. O. S. Lee, and S. V Patankar, "Treatment of irregular geometries using a Cartesian coordinates finite-volume radiation heat transfer procedure," *Numer. Heat Transf. Part B Fundam.*, vol. 26, no. 2, pp. 225–235, Sep. 1994, doi: 10.1080/10407799408914927.

[38] S. a. L. Glegg, C. Jochault, J. C. Chai, H. S. Lee, and S. V. Patankar, "Finite volume method for radiation heat transfer," *J. Thermophys. Heat Transf.*, vol. 8, no. 3, pp. 419–425, 1994, doi: 10.2514/3.559.

[39] V. I. Lebedev V. A. Sokolov, "Multiple heat exchange in a model furnace with direct heating," *Glas. Ceram.*, vol. 37, no. 2, pp. 67–69, 1980.

[40] V. I. Lebedev V. A. Sokolov, "Study of the convection component of complex heat exchange in a model of a direct-heating furnace," *Glas. Ceram.*, vol. 35, no. 6, pp. 352–354, 1976.

[41] J. C. Chai, *A general-purpose computer program for Radiative Transfer, RAT, Version 1*. 2003.

[42] A. Emadi, A. Saboonchi, M. Taheri, and S. Hassanpour, "Heating characteristics of billet in a walking hearth type reheating furnace," *Appl. Therm. Eng.*, vol. 63, no. 1, pp. 396–405, 2014, doi: 10.1016/j.applthermaleng.2013.11.003.